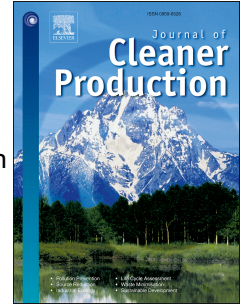


# Journal Pre-proof

Fast fatigue method for self-compacting recycled aggregate concrete characterization

Jose Sainz-Aja, Carlos Thomas, Isidro Carrascal, Juan A. Polanco, Jorge de Brito



PII: S0959-6526(20)33308-4

DOI: <https://doi.org/10.1016/j.jclepro.2020.123263>

Reference: JCLP 123263

To appear in: *Journal of Cleaner Production*

Received Date: 1 April 2020

Revised Date: 23 June 2020

Accepted Date: 10 July 2020

Please cite this article as: Sainz-Aja J, Thomas C, Carrascal I, Polanco JA, de Brito J, Fast fatigue method for self-compacting recycled aggregate concrete characterization, *Journal of Cleaner Production*, <https://doi.org/10.1016/j.jclepro.2020.123263>.

This is a PDF file of an article that has undergone enhancements after acceptance, such as the addition of a cover page and metadata, and formatting for readability, but it is not yet the definitive version of record. This version will undergo additional copyediting, typesetting and review before it is published in its final form, but we are providing this version to give early visibility of the article. Please note that, during the production process, errors may be discovered which could affect the content, and all legal disclaimers that apply to the journal pertain.

© 2020 Elsevier Ltd. All rights reserved.

1  
2  
3  
4  
5  
6  
7  
8  
9  
10  
11  
12

## **Fast fatigue method for self-compacting recycled aggregate concrete characterization**

*Jose Sainz-Aja<sup>1</sup>, Carlos Thomas<sup>1\*</sup>, Isidro Carrascal<sup>1</sup>, Juan A. Polanco<sup>1</sup>, Jorge de Brito<sup>2</sup>*

<sup>1</sup>LADICIM (Laboratory of Materials Science and Engineering), Universidad de Cantabria. E.T.S. de Ingenieros de Caminos, Canales y Puertos, Av./Los Castros 44, 39005 Santander, Spain.

<sup>2</sup>CERIS, Instituto Superior Técnico, Universidade de Lisboa, Av. Rovisco Pais, 1049-001 Lisbon, Portugal.

\* Corresponding author: carlos.thomas@unican.es

# Fast fatigue method for self-compacting recycled aggregate concrete characterization

Jose Sainz-Aja<sup>1</sup>, Carlos Thomas<sup>1\*</sup>, Isidro Carrascal<sup>1</sup>, Juan A. Polanco<sup>1</sup>, Jorge de Brito<sup>2</sup>

<sup>1</sup>LADICIM (Laboratory of Materials Science and Engineering), Universidad de Cantabria. E.T.S. de Ingenieros de Caminos, Canales y Puertos, Av./Los Castros 44, 39005 Santander, Spain.

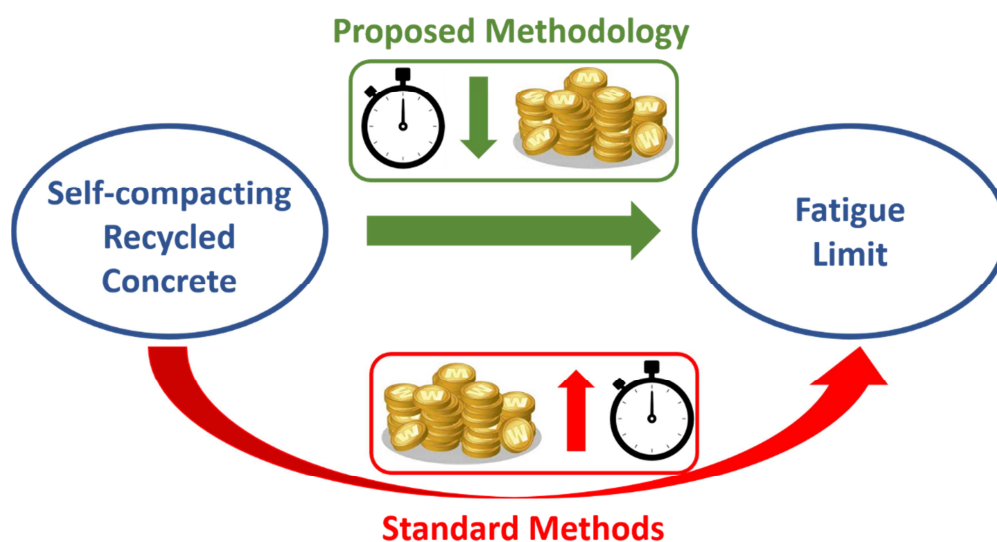
<sup>2</sup>CERIS, Instituto Superior Técnico, Universidade de Lisboa, Av. Rovisco Pais, 1049-001 Lisbon, Portugal.

\* Corresponding author: carlos.thomas@unican.es

## Abstract:

Designing or analysing the influence of fatigue on concrete structures is becoming increasingly important for a number of structural elements. For this reason, it is necessary to define a method capable of determining the concrete's fatigue limit in the most economical, fast and efficient way. The aim of this study is to compare and correlate different methods found in the literature in order to reduce the number and duration of the tests required to determine the fatigue limit. This reduction will consequently reduce the economic costs of determining the fatigue limit. For these purposes three different types of self-compacting recycled concrete was used. A linear correlation was found between the analysed methods, which means that the methods are capable of providing similar results and that the results obtained by the economical procedure must be selected. This work opens the door to define an optimal procedure in the process of concrete fatigue characterization, which is capable of yielding results up to five times faster and more economical **than with other methodologies**, so that resources are not wasted.

**Keywords:** resonance frequency; recycled aggregate; recycled aggregate concrete; fatigue; Locati; Staircase; self-compacting



**29 Highlights:**

- 30 • Locati and Staircase method provide similar fatigue limit in high frequency fatigue;
  - 31 • A drop in the resonance frequency means an increased damage;
  - 32 • 2×10<sup>5</sup> cycles per Locati step are enough to determine the fatigue limit.
- 33

**34 1. Introduction**

35 Concrete is the material most used in construction sector. In addition, approximately 10% of  
36 man-made CO<sub>2</sub> emissions are from concrete production and transportation (Sainz-Aja et al., 2020) and,  
37 for this reason, there are numerous studies that seek ways to reduce concrete's environmental impact.  
38 Naseri et al. (2020) developed a new machine learning technique to design sustainable concrete mixes.  
39 Zhao et al. (2020) used a ternary diagram to compare traditional concrete with three kinds of green  
40 concrete: recycled aggregate concrete production mode, fly ash concrete production mode, and  
41 circular economy concrete production mode, the importance of the circular economy is highlighted by  
42 other authors such as Maroušek et al. (2019). Opon and Henry (2019) defined a new indicator to  
43 quantify the sustainability of concrete. This new indicator considers the pillars of sustainability  
44 (environment, economy and society) and the sustainable development goal. Marvila et al. (2019)  
45 checked the possibility of total replacing all or at least a part of hydrated lime with marble waste.  
46 Azevedo et al. (2020) evaluated a new process methodology trying to incorporate primary pulp and  
47 paper industry sludge waste into cement and lime-base mortars. But, nowadays, the most popular  
48 way to try to reduce concrete environmental impact is to use recycled aggregates (RA) instead of  
49 natural aggregates.

50 It has been widely established that the use of RA is a necessity nowadays because of the large  
51 amount of waste going to landfill every day (Poon and Chan, 2007). This environmental concern is  
52 mitigated by ensuring that these wastes can generate concrete with both good mechanical (Thomas  
53 et al., 2013) and durability (Thomas et al., 2013) properties.

54 While the fatigue behaviour of structural metal elements is commonly studied, in the case of  
55 concrete elements it is not so common. Although it is not usual to carry out a fatigue characterisation of  
56 concrete elements, there are some elements that are subject to highly variable significant loads that  
57 make it necessary to perform fatigue characterisation. Examples of this type of elements include:  
58 offshore structures subject to variable wind, waves and tidal loads (Xiao et al., 2013), rail and road  
59 bridges (Alliche, 2004), railway superstructures, sleepers (Ferreño et al., 2019) or slab tracks (Sainz-Aja  
60 et al., 2020) and/or wind generators (Skarżyński et al., 2019). This is why several authors have  
61 performed studies that analyse the fatigue behaviour of concrete at the microstructural level by means  
62 of tomographic analysis (Thomas et al., 2019, 2018), even establishing the concrete fatigue  
63 micro-mechanisms that produce concrete failure with recycled (Sainz-Aja et al., 2019a) and natural  
64 aggregates (Skarżyński et al., 2019), Thomas et al. (2014) determined the fatigue limit under  
65 compression of 24 mix proportions of RAC. Xiao et al. (2013) analyzed the effect of compressive and  
66 bending fatigue of recycled aggregate concrete. Li et al. (2016) analyzed the compressive fatigue  
67 behavior of fiber reinforced cementitious materials. Vicente et al. (2019) analyzed the bending fatigue  
68 using computed tomography scanning. From these studies, it was possible to define the damage  
69 procedure undergone by concrete until its failure. This process begins with the onset of cracks in the  
70 interfacial transition zone (ITZ). Subsequently, these cracks begin to grow and interconnect until they  
71 reach a critical dimension that leads to failure (Carloni and Subramaniam, 2013). Regarding the fatigue  
72 behaviour of recycled concrete, although it is not a very developed topic, there are some works that  
73 indicate that the use of recycled concrete aggregates reduces the fatigue life, especially at replacements  
74 greater than 20% (Luo and Yao, 2011). Thomas et al. (2014) determined that the loss in the fatigue limit  
75 due to the presence of recycled aggregates is higher than the reduction in the compressive strength.  
76 Also, Thomas et al. (2014) found that the effect of the recycled aggregate on the concrete dynamic  
77 response depends not only on the quality of the recycled aggregate but also the new concrete quality.

78 Strength-Number of cycles' (S-N) curves are the most common way of analysing fatigue  
79 behaviour. Moreover, this is the method proposed by Eurocode 2 (British Standards Institution,  
80 2015). However, the problem with this methodology is that it requires a large number of long-term  
81 tests and specimens, which means both an increase in time and a high economic cost and, in some  
82 cases, it is not possible to provide these samples. In addition to the S-N curves, a number of other  
83 characterisation techniques that focus on determining the fatigue limit only have been taken into  
84 account. Fatigue limit is the threshold stress range below which failure does not occur  
85 independently of the number of cycles applied, so that infinite life can be considered in relation to  
86 these stress levels. Specifically, the Staircase method has been proposed. This testing methodology is  
87 used as a standardized procedure, for e.g. to characterize the fatigue limit in welded rails, according  
88 to standard UNE-EN 14587-1 (CEN, 2018). This type of test requires a significantly lower number of  
89 tests than those required to determine an S-N curve, but approximately 10 results are still required.  
90 In order to shorten the time and lower the economic cost and the number of samples required,  
91 another test method, the Locati method, was used (Locati, 1950), which intends to estimate the  
92 fatigue limit by means of a single test. A procedure similar to the Locati method is used as a  
93 standardized procedure to determine the fatigue limit of railway sleepers (CEN, 2016).

94 The Locati method has been used by different researchers to determine the fatigue limit,  
95 although there is no unanimity in the procedure to determine the fatigue limit of the Locati tests.  
96 Kong et al. (2015) analysed the effect of laser quenching on fatigue properties and fracture  
97 morphologies of boronized layer on Cr12MoV Steel by Locati method. They determine the fatigue  
98 limit by fatigue accumulation damage. Maximov et al. (2017) analysed the effect of slide burnishing  
99 on the high-cycle fatigue performance of 2024-T3 high-strength aluminium alloy by the Locati  
100 method. The fatigue limit was determined assuming the validity of Palmgren–Miner linear damage  
101 hypothesis. Sainz-Aja et al. (2019a) used the Locati method to determine the fatigue failure  
102 micro-mechanisms in recycled aggregate mortar combined with  $\mu$ CT analysis. Sainz-Aja et al.  
103 (2019c) used the Locati method to determine the fatigue limit of high-frequency tests of recycled  
104 aggregate concrete. In this case, the parameter to determine the fatigue limit was a decrease in the  
105 fatigue resonance frequency. Casado et al. (2006) used the Locati method to determine the Fatigue  
106 failure of short glass fibre reinforced PA 6.6 structural pieces for railway track fasteners. In this case,  
107 the fatigue limit was determined based on the strain evolution. Thomas et al. (2014) used the Locati  
108 method to determine the recycled aggregate concrete fatigue behaviour. They determined the  
109 fatigue limit as a correlation with the maximum load of the Locati tests.

110 Conventionally, the Staircase method at constant and moderate frequency is the way to  
111 determine concrete's fatigue limit, but is it the best way to determine it? The aim of this work is to  
112 validate a method to determine the concrete fatigue limit ( $\Delta\sigma_{FL}$ ) and the fatigue limit/compressive  
113 strength ratio ( $\Delta\sigma_{FL}/f_c$ ) with the least number of test specimens and in the shortest possible time. For this  
114 purpose, the test frequency was increased as much as possible to compare the Staircase and Locati  
115 methods and characterize three recycled concrete types. Fatigue tests were performed in a resonance  
116 compression fatigue test machine, which performs tests at the resonance frequency of the assembly  
117 test machine and specimen, in this case approximately 90 Hz. Regarding the test, the Staircase method  
118 was taken as a reference with  $2 \times 10^6$  cycles per test (Bellido de Luna, 1989), which was compared with  
119 Locati tests. As there is no certainty about the number of cycles per step in the Locati method, it was  
120 decided to perform it, on the one hand, with  $2 \times 10^5$  (L2) and, on the other hand,  $5 \times 10^5$  (L5) cycles per  
121 step, thus enabling the analysis of the influence of the number of cycles per step. Finally, the influence  
122 of the material was analysed, characterising three types of self-compacting recycled concrete, the first  
123 of which made with recycled aggregate from out-of-use railway ballast (RC-B), which is similar to  
124 natural aggregate. The second one was made from recycled aggregate from out-of-use railway sleepers  
125 (RC-S), i.e. recycled concrete aggregate. The third one contained both types of aggregate, ballast and  
126 out-of-use sleepers, in the proportions in which they are found in tracks (RC-M).

127 In this paper, once the introduction is finished, in the section of Materials and methodology, the  
128 materials used in the research, the mix proportions of concrete and the procedures followed to obtain  
129 compressive strength, elastic modulus and the three types of fatigue tests carried out are described in

130 detail. The following section, "Results and discussions", is divided into three blocks: results of  
 131 compressive strength and elastic modulus tests, results of the fatigue tests, and an analysis of the  
 132 correlation between the different methods used to determine the fatigue limit. Finally, the conclusions  
 133 obtained from this work are presented.

## 134 2. Materials and methodology

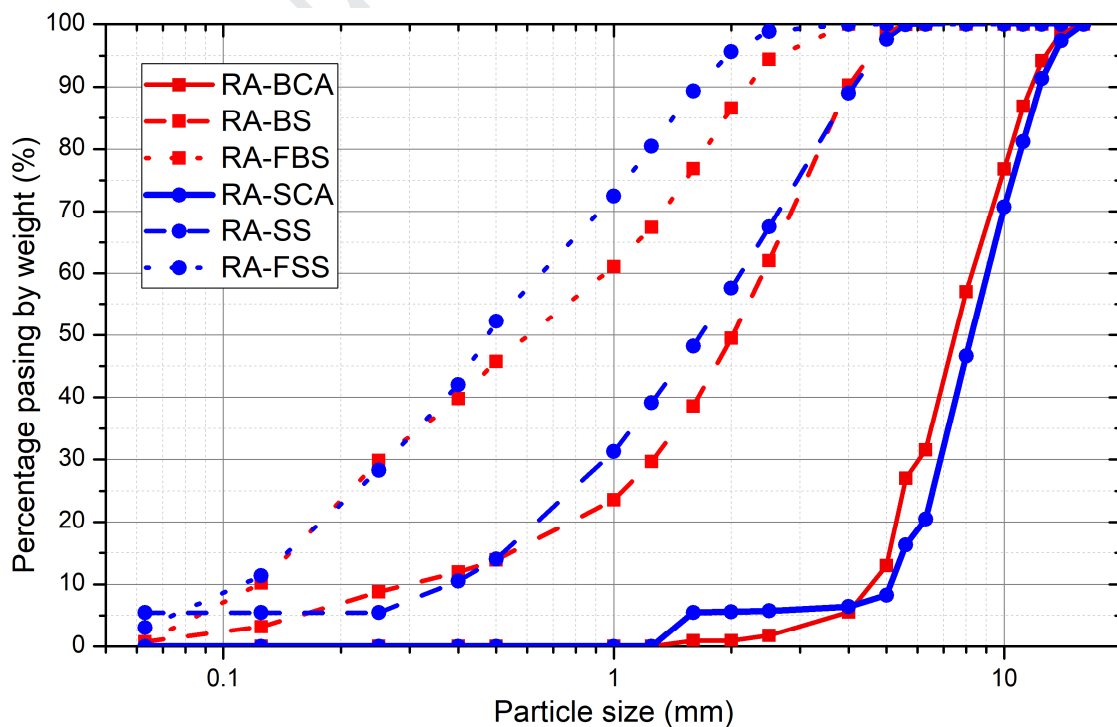
135 The design of experiments proposed for this research begins with the characterization of the  
 136 aggregates and cement. Afterwards, three mix proportions of recycled self-compacting concrete are  
 137 defined. Subsequently, the values of compressive strength and elastic modulus are determined, and  
 138 the fatigue tests end the procedures. These fatigue tests include Staircase tests as Locati tests with  
 139  $2 \times 10^5$  and  $5 \times 10^5$  cycles per step.

### 140 2.1. Aggregates

141 The three self-compacting recycled concrete mixes were manufactured using exclusively  
 142 recycled aggregates from the valorisation of out-of-service railways superstructure, ballast (RA-B)  
 143 and sleepers (RA-S). These wastes were crushed and sieved, grouping each of the wastes in three  
 144 size fractions. Table 1 shows the classification and the relative density of coarse aggregates and the  
 145 real density of sands. Fig. 1 shows the grading curve of each of the aggregates. Moreover, the  
 146 flakiness indexes of the coarse aggregates (CA) were: 14 % for RA-B-CA and 5 % for RA-S-CA. The  
 147 water absorption coefficient of RA-B-CA in 1.9 % and 5.1% wt. for the RA-S-CA.

148 *Table 1: Aggregate properties.*

Description	Code	Min-Max size (mm)	Density (g/cm <sup>3</sup> )
Ballast coarse aggregate	RA-B-CA	5-12	2.57
Sleeper coarse aggregate	RA-S-CA	5-12	2.38
Ballast coarse sand	RA-B-LS	2-5	2.74
Sleeper coarse sand	RA-S-LS	2-5	2.45
Ballast fine sand	RA-B-FS	0-2	2.82
Sleeper fine sand	RA-S-FS	0-2	2.51



150 *Fig. 1: Aggregate grading curves. The recycled aggregates from crushed sleepers are represented in blue*  
 151 *and the ones from crushed ballast in red.*

## 152 2.2. Cement

153 As a self-compacting concrete needs a high volume of fine particles and the recycled sands were  
 154 not able to provide this, a CEM IV (V) 32.5 N type cement according to EN 197-1 (CEN, 2011a) was  
 155 used, which has a high replacement of clinker with fly ash. The density of this cement according to  
 156 UNE 80103 (CEN, 2013) is 2.85 g/cm<sup>3</sup>. The Blaine specific surface is 3885 cm<sup>2</sup>/g according to EN 196-6  
 157 (CEN and 196-6:2010, 2010). Table 2 shows the cement's chemical composition by fluorescence.

158 *Table 2: Cement chemical composition.*

	Composition (% wt.)							
	CaO	SiO <sub>2</sub>	Fe <sub>2</sub> O <sub>3</sub>	Al <sub>2</sub> O <sub>3</sub>	MgO	K <sub>2</sub> O	SO <sub>3</sub>	Ignition loss
CEM IV	35.5	41.2	4.4	13.3	1.2	1.4	1.3	1.7

## 159 2.3. Mix proportions

160 Three concrete mix proportions were designed. The first one, RC-B, used only recycled  
 161 aggregates from crushed ballast, the second one, RC-S, used exclusively recycled aggregates from  
 162 out-of-service sleepers, and finally, the third one, RC-M, using both kinds of aggregates in the  
 163 proportion that they occur in the track, 6/7 of ballast and 1/7 of sleepers. Table 3 shows the three mix  
 164 proportions.

165 *Table 3: Mix proportions (kg/m<sup>3</sup>).*

Material	RC-B	RC-S	RC-M
Water	225	200	221
Cement	500	500	500
Superplasticizer additive	10	10	10
RA-B-FS	790	-	677
RA-B-LS	320	-	274
RA-BCA	522	-	447
RA-S-FS	-	690	98
RA-S-LS	-	283	40
RA-S-CA	-	587	83
% sand (0-2 mm) of the total sand	70	70	70
% coarse aggregate of the total aggregates	35	40	36
Water/cement ratio	0.45	0.40	0.44
% superplasticizer additive/cement	2.00	2.00	2.00

166 The mix proportions were tuned to obtain a similar workability in the three mixes. For this  
 167 reason, it was necessary to increase the water content of RC-B, due to RA.B's higher flakiness index  
 168 (Sainz-Aja et al., 2019b). A high content of fine aggregates in the mix proportion was needed to obtain  
 169 self-compacting features. The superplasticizer admixture used in this work is a polycarboxylic ether  
 170 type superplasticizer called "MasterGlenium® ACE 450 BASF"  
 171

## 172 2.4. Mechanical properties

173 The evolution over time of the two main mechanical properties of concrete, compressive  
 174 strength and Young's modulus, was measured. For compressive strength characterization, 100 mm  
 175 cubes were tested according to the EN 12390-3 and EN 13290-3/AC (CEN, 2011b; CEN et al., 2009)  
 176 standards at 1, 2, 3, 5, 7, 28, 90 and 180 days. Modulus of elasticity tests were carried out at 7, 28, 90  
 177 and 180 days, according to EN 12390-13 (CEN, 2014) and using cylindrical test specimens of 200 mm



210

$$A = \sum i \cdot n_i \quad \text{Equation 1}$$

$$N = \sum n_i \quad \text{Equation 2}$$

$$B = \sum i^2 \cdot n_i \quad \text{Equation 3}$$

$$\sigma'_{FL} = \sigma_0 + \delta \cdot \left( \frac{A}{N} \pm 0.5 \right) \quad \text{Equation 4}$$

211 Once the parameters N, A and B have been determined, using Equation 6 it is possible to  
 212 determine the fatigue limit of the samples analysed. In Equation 4,  $\sigma_0$  is the stress range of the  
 213 reference step,  $\delta$  is the variation of stress range between successive steps and  $\pm$  is plus (+), if the less  
 214 usual event is that it exceeds the step and, less (-), if on the contrary, the less usual event is that it  
 215 does not exceed the step. The standard deviation (S) is equal to Equation 5 if Equation 7 is met.

$$S = 1.62 \cdot \delta \cdot \left( \frac{B \cdot N - A^2}{N^2} + 0.029 \right) \quad \text{Equation 5}$$

$$\sigma_{FL} = \sigma'_{FL} \pm S \text{ (MPa)} \quad \text{Equation 6}$$

$$\frac{B \cdot N - A^2}{N^2} > 0.3 \quad \text{Equation 7}$$

216

*Table 5: Fatigue test stress scenarios.*

Step	k	RC-B			RC-S			RC-M		
		$\sigma_{Max}$ (MPa)	$\sigma_{Min}$ (MPa)	$\Delta\sigma$ (MPa)	$\sigma_{Max}$ (MPa)	$\sigma_{Min}$ (MPa)	$\Delta\sigma$ (MPa)	$\sigma_{Max}$ (MPa)	$\sigma_{Min}$ (MPa)	$\Delta\sigma$ (MPa)
1	0.30	17.8	1.8	16.0	23.3	2.3	21.0	18.9	1.9	17.0
2	0.35	20.8	2.1	18.7	27.2	2.7	24.5	22.0	2.2	19.8
3	0.40	23.8	2.4	21.4	31.1	3.1	28.0	25.1	2.5	22.6
4	0.45	26.7	2.7	24.0	35.0	3.5	31.5	28.3	2.8	25.5
5	0.50	29.7	3.0	26.7	38.9	3.9	35.0	31.4	3.1	28.3
6	0.55	32.7	3.3	29.4	42.8	4.3	38.5	34.6	3.5	31.1
7	0.60	35.7	3.6	32.1	46.7	4.7	42.0	37.7	3.8	33.9
8	0.65	38.6	3.9	34.7	50.6	5.1	45.5	40.8	4.1	36.7
9	0.70	41.6	4.2	37.4	54.5	5.4	49.1	44.0	4.4	39.6

217

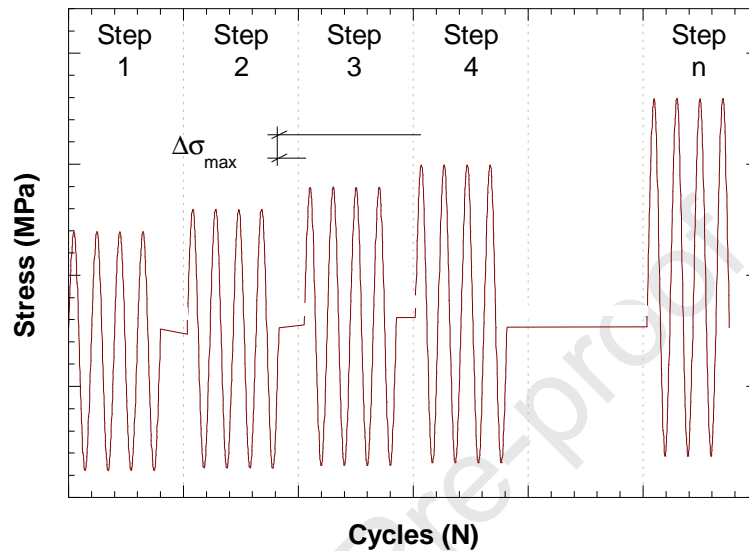
218 The Locati method seeks to estimate the fatigue limit using a single test specimen, thus reducing the  
 219 number of tests will reduce the overall cost of the tests. For this purpose, the test procedure consists of  
 220 applying increasing load steps, with a fixed number of cycles per step, until the specimen breaks. An  
 221 explanatory diagram can be seen in Fig. 3. In this case, the load steps were defined previously in Table 5  
 222 and, as commented upon in the introduction, because there is no standard in which the number of cycles  
 223 per Locati method step is specified, it was decided to perform and compare L2 and L5. Different authors  
 224 use different criteria to estimate the fatigue limit through the Locati test (Casado et al., 2006; Kong and  
 225 Xie, 2015; Maximov et al., 2017; Sainz-Aja et al., 2019a, 2019c; Carlos Thomas et al., 2014). In this situation,  
 226 to analyse the Locati method, two criteria found in the literature were used: method-1 and method-2.  
 227 Method-1, proposed by Thomas (2012) in his PhD thesis, defines the fatigue limit as 80% of the stress  
 228 range of the last step that the specimen withstands. Method-2, proposed by Sainz-Aja (2019) in his PhD

229 thesis, defines the fatigue limit in resonance as the stress range of the step previous to the step in which a  
 230 fall in resonance frequency of the system is observed.

### 231 3. Results and discussions

#### 232 3.1. Compressive strength and Young's modulus

233 Table 6 shows the evolution of compressive strength and Young's modulus as a function of  
 234 time.



235

236 *Fig. 3: Locati test example where five different steps can be seen. The first four consecutively and the fifth*  
 237 *corresponding to a step "n".*

238

**Table 6: Mechanical properties.**

Property	Compressive strength (MPa)				Young's modulus (GPa)			
Age (days)	7	28	90	180	7	28	90	180
RC-B	32.5	49.4	59.4	66.2	26.4	30.5	33.4	35.3
RC-S	41.9	57.2	77.8	82.3	26.1	28.9	33.2	34
RC-M	37.6	52.6	62.8	70.4	25.5	31.6	32.2	35.2

239

240 The evolution on the compressive strength shows the great influence of w/c ratio on  
 241 compressive strength, which is the reason why the compressive strength of RC-S is higher than that  
 242 of RC-B in spite of having poorer quality aggregates. Furthermore, the effect of the fly ash contained  
 243 in CEM type IV is noticeable, as it causes the resistance to increase notably after 28 days. It can also  
 244 be seen that the strength of RC-M is in all cases between those of RC-B and RC-S (Sainz-Aja, 2019).

245 In the case of the Young's modulus, due to the higher stiffness of the crushed ballast aggregates,  
 246 the corresponding concrete's stiffness is also higher, although the mortar quality of RC-B is lower  
 247 than that of RC-S because of the difference in the w/c ratio.

#### 248 3.2. Staircase test results

249 First, the Staircase tests were used to obtain the fatigue limit by means of the standardized  
 250 Staircase procedure, the results of which are shown in Table 7.

251

**Table 7: Fatigue limit according to the Staircase tests.**

Material	$\Delta\sigma_{FL}$ (MPa)	$\Delta\sigma_{FL}'$ (%)
RC-B	28.1±2.7	47.4±4.5

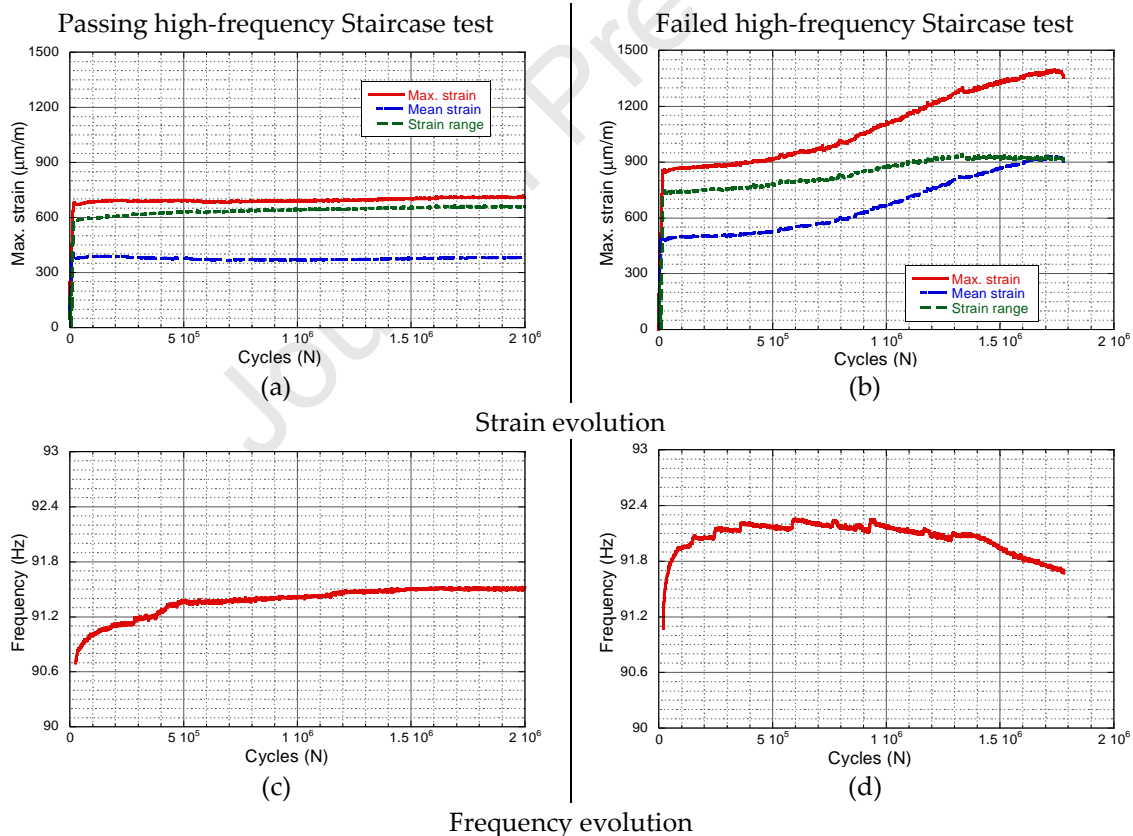
RC-S	28.0±3.5	36.1±4.5
RC-M	27.8±2.8	44.1±4.5

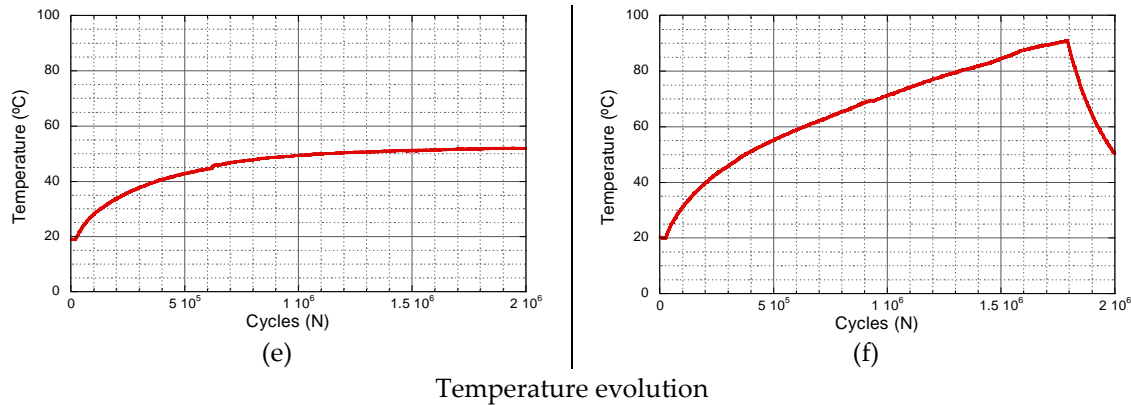
252  
253  
254  
255  
256  
257  
258  
259  
260  
261  
262  
263  
264  
265  
266  
267  
268  
269

The fatigue limits of the three concrete mixes are similar. If the ratio fatigue limit/compressive strength is analysed, a reduction can be seen in RC-S caused by the presence of recycled concrete aggregates. This reduction in this ratio has been previously detected by other authors (Sainz-Aja et al., 2019c; Thomas et al., 2014).

To understand as well as possible the phenomenon that produces fatigue failure in concrete, the values of strain, resonance frequency and temperature were registered throughout the test. Fig. 4 (a), (c) and (e) show a test case where a specimen successfully passes the Staircase test step, while Fig. 4 (b), (d) and (f) show a test case where the specimen does not pass the step.

Regarding concrete strain evolution, when the specimen passes, a stabilization of the maximum, mean and strain range is observed after a few cycles. When the specimen does not pass, strain starts to grow increasingly faster until it breaks, which is consistent with previous observations (Li et al., 2016; Sainz-Aja et al., 2019c). Regarding the resonance frequency evolution, when the specimen passes, the resonance frequency stabilizes, while when the specimen does not pass, the frequency increases in a first phase, after which it is more or less stable until the final stage, when it starts to decrease before breaking, which is also consistent with previous observations (Sainz-Aja et al., 2019c).



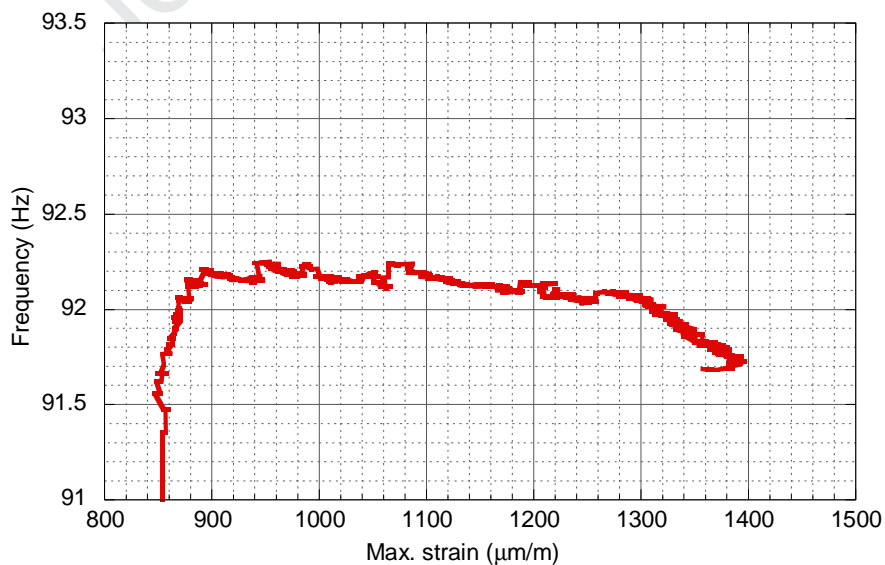


270 **Fig. 4:** Comparison of a passing with a failed high frequency Staircase test (RC-M). The same phenomenon has  
 271 been represented in three different ways. Firstly, evolution of strain, secondly frequency and finally  
 272 temperature, all of them against the number of fatigue cycles.

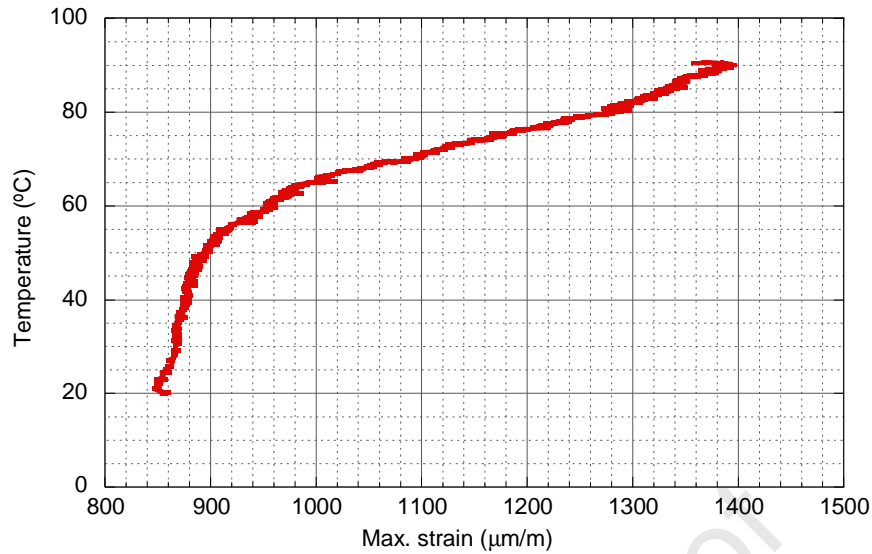
273 Regarding the temperature evolution of the external surface of the specimen, when the  
 274 specimen passes, similarly to the deformation and frequency, temperature will stabilize, at  $60 \pm 5$  °C  
 275 in all cases. When the specimen does not pass, in contrast to what happens with frequency or  
 276 deformation, two types of behaviour occur depending on whether the test specimen breaks within  
 277 the first phase of the step or, on the contrary, it withstands most of it. It has been found that in the  
 278 first case, the increase in temperature can be significantly variable, while if it withstands enough  
 279 cycles, the temperature values of the external face of the specimen rise to approximately 100 °C. This  
 280 phenomenon is observed for the three concrete mixes. This increase in specimen temperature may be  
 281 due to fatigue friction between the contacting faces of the fissures, generating energy.

282 The difference between low and high frequency is that in high-frequency tests the time between  
 283 cycles is not sufficient to dissipate the heat generated by that friction, so the energy is accumulated in  
 284 the specimen, continuously increasing the temperature until failure. When the friction stops, the  
 285 temperature begins to fall. For specimens that break after a few cycles, they accumulate this energy  
 286 for a short time, so its temperature may not increase as much as when they withstand more cycles.

287 In addition, focusing on the failing tests, the evolution of both temperature and test frequency  
 288 as a function of strain can be seen in Fig. 5 and Fig. 6.



289 **Fig. 5:** Evolution of resonance frequency as a function of max. strain during high-frequency fatigue failure (RC-M).  
 290 Result of the variation by automatic adjustment of the resonance frequency during the Staircase test, allowing  
 291 observing the initial increase and the decrease with the loss of stiffness of the material.  
 292



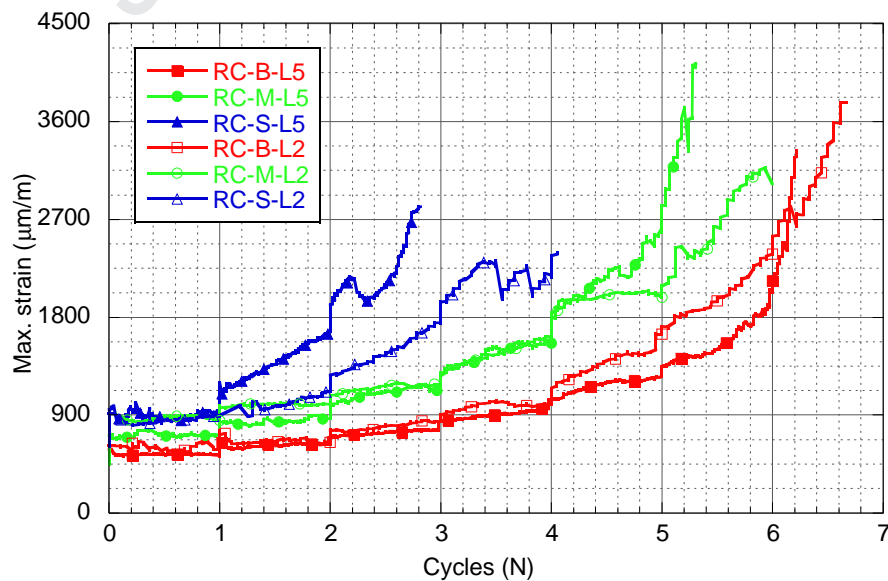
293

294 **Fig. 6:** Evolution of temperature as a function of max. strain during high-frequency fatigue failure (RC-M). A  
 295 continuous increase of temperature by accumulation of energy due to fatigue cycles is observed.

296 Fig. 5 and Fig. 6 show that there is a first stage, when strain reaches approximately 900  $\mu\text{m/m}$ . For  
 297 resonance frequency, up to that point it increases with the increase in strain, while from that point on it  
 298 starts to fall. For temperature, up to 900  $\mu\text{m/m}$  its growth is much faster than from that point on. In  
 299 addition, it can also be observed that, at the point that marks this change in trend, the external face is  
 300 above 60 °C. When the temperature exceeds that range of temperature, the test specimen is close to  
 301 breaking.

### 302 3.3. Locati test results

303 To be able to compare the Locati method with the Staircase method, it is necessary to check that the  
 304 number of Locati cycles applied per step is suitable. For this purpose, Locati tests were carried out  
 305 applying  $2 \times 10^5$  and  $5 \times 10^5$  cycles per step and the results of L2 and L5 were compared and similar results  
 306 were obtained. Fig. 7 shows the maximum strain of an example of each binomial material & number of  
 307 cycles per step. Fatigue limit results, according to the two methods described in materials and methods,  
 308 are presented in Table 8.



309

310 **Fig. 7:** Example of maximum strain for each binomial material & number of cycles per Locati step. Its evolution  
 311 is represented by different colours: red for RC-B, green for RC-M and blue for RC-S.

312

*Table 8: Fatigue limit according to Locati tests.*

Material	Method-1		Method-2	
	$\Delta\sigma_{FL}$ (MPa)	$\Delta\sigma_{FL}'$ (%)	$\Delta\sigma_{FL}$ (MPa)	$\Delta\sigma_{FL}'$ (%)
RC-B-L5	24.6±2.7	43.2±4.5	26.7±2.7	45.1±4.5
RC-S-L5	23.8±3.5	30.7±4.5	24.5±3.5	31.5±4.5
RC-M-L5	23.7±2.8	37.7±4.5	25.5±2.8	40.5±4.5
RC-B-L2	25.7±2.7	45.1±4.5	26.7±2.7	46.9±4.5
RC-S-L2	25.2±3.5	32.4±4.5	28.0±3.5	36.1±4.5
RC-M-L2	24.9±2.8	39.5±4.5	28.3±2.8	44.9±4.5

313

314

315

316

317

Comparing the fatigue limit results and maximum strain values of the two types of Locati tests, the L2 results are more conservative than those of L5, but that the difference between them, in the worst case, is one Locati step. So, due to the inherent dispersion of both concrete and fatigue, it can be considered that the methods provide similar results.

318

#### 3.4. Correlation of methods

319

320

321

In this section, the fatigue limit values for all methods, are compared. Fig. 8 shows the five fatigue limits obtained by those different methods on the left, while, on the right, the five values of fatigue limit/compressive strength are compared.

322

323

324

In all cases method-1 is more conservative than method-2. If the results L2 and L5 are compared, in all cases L5 is more conservative. Finally, in all cases the Locati method is more conservative than the Staircase method.

325

326

327

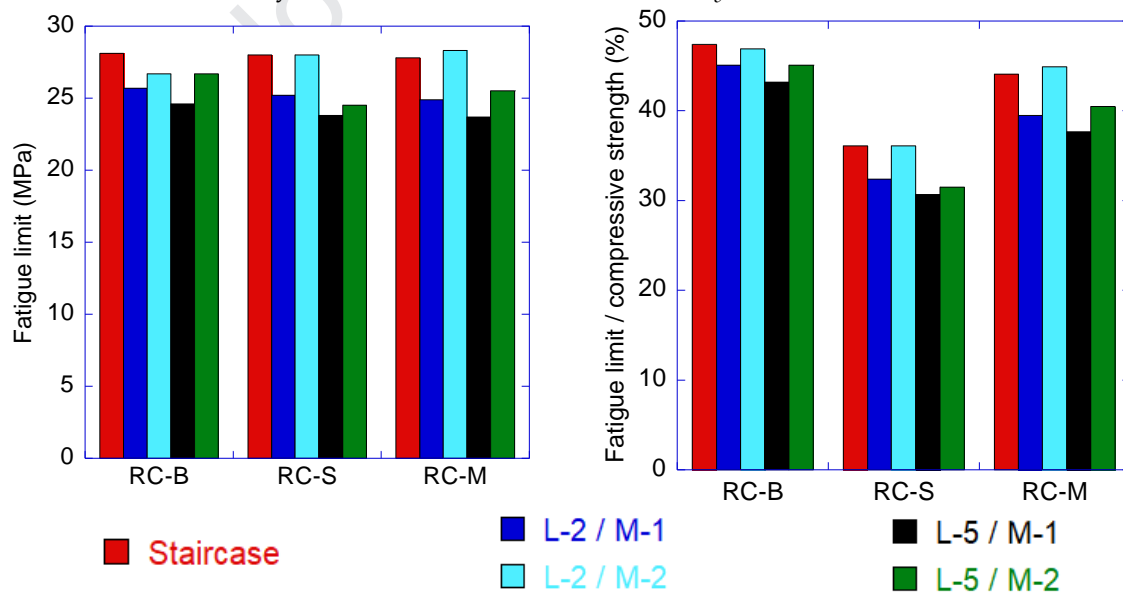
328

Using the Staircase method as reference given that it is the standardized and most used method, it is possible to state that the Locati method gives in all cases more conservative, but quite similar results, and those analysed through L-2/M-2 provide the closest results to those obtained by the Staircase method.

329

330

In Fig. 9, the fatigue limit value obtained by the Staircase method is shown in the x axis while the value determined by the Locati methods is shown in the y axis.

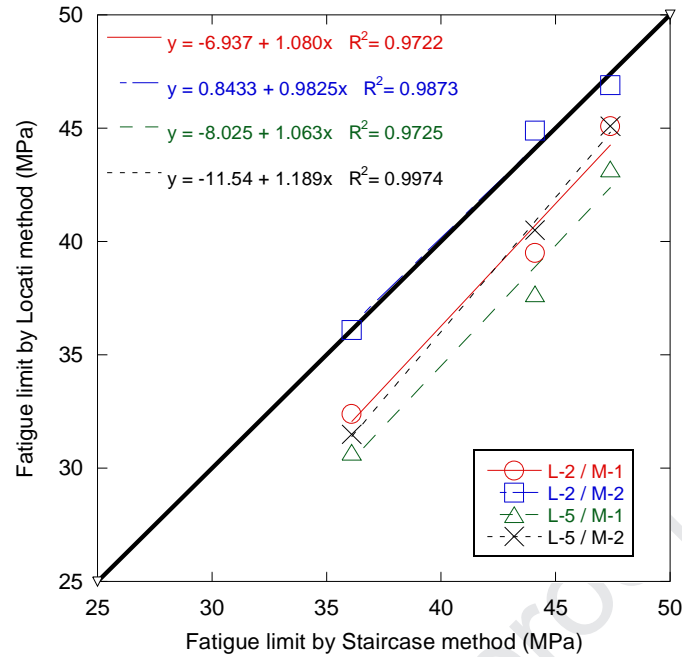


331

332

333

*Fig. 8: Comparison of the high-frequency fatigue limit and of the low-frequency fatigue limit, obtained through five alternative procedures. The control test is shown in red and those proposed in this research are shown in blue, black and green.*



334  
335  
336

*Fig. 9: Correlation Staircase vs. Locati method. All the adjustment lines are below the 45-degree line, the furthest being the green one corresponding to the L-5 / M1 case.*

337  
338  
339  
340  
341  
342  
343  
344

From Fig. 9, it can be concluded the results provided by the Locati method and the Staircase method are proportional. Note that the slope of all the regression lines, except for L-5/M-2, is  $1 \pm 0.08$ . Also, the parameters used to define the Locati test, number of cycles per step, and analysis procedure, have some influence on the correlation between the fatigue limit obtained by both methods. For L-2/M-2, the results are practically the same in both methods, and L-2/- 1, L-5/M-1 and L-5/M-2 are more conservative. It can also be concluded that method 1 is more conservative than method 2 and applying  $2 \times 10^5$  cycles per step is more conservative than applying  $5 \times 10^5$  cycles per step.

345

#### 4. Costs-related remarks

346  
347  
348  
349  
350

A reduction in the number of tests will have a consequent economic cost reduction in the fatigue characterization of the recycled concrete. In general, fatigue characterization tests are budgeted according to the machine hours required to perform the tests. As the testing time is directly related to the testing frequency, in this point it will be only compare the effect of using the Locati method instead of the Staircase method, without analyzing the effect of the frequency.

351  
352  
353  
354  
355

The characterization time for Locati tests will be approximately 7 steps of  $2 \times 10^5$  cycles, performing two tests per material. In the case of characterization by the Staircase method, there will be a total of at least 9 tests, of which approximately 50% will reach  $2 \times 10^6$  cycles and, let us assume that the other 50% will remain at  $1 \times 10^6$  cycles. Under these assumptions, the characterization by the Staircase method is almost 5 times higher than by the Locati method.

356

#### 5. Conclusions

357  
358  
359  
360  
361  
362  
363  
364

The importance of designing concrete elements bearing fatigue in mind is becoming increasingly clear. For this reason, it is essential to identify a method that allows determining concrete fatigue limit as fast, economically and accurately as possible. In order to achieve this objective, two test methods have been compared in this work, the standardised Staircase method and a method that proposes determining fatigue limit from a single test specimen, the Locati method. In addition, the number of cycles per step, in the Locati method, was analysed through testing. These fatigue tests were performed on three self-compacting recycled concrete types. The first one used recycled aggregate from crushed ballast, which has a similar behaviour to natural

365 aggregate. The second one used recycled aggregate from crushed concrete sleepers. Finally, a third  
366 concrete had 6/7 of aggregate from crushed ballast and 1/7 of aggregate from crushed sleepers. In  
367 order to reduce the duration and, consequently, the cost of the fatigue tests as much as possible,  
368 these tests were carried out in a resonance machine at a frequency of approximately 90 Hz. The  
369 following conclusions can be drawn:

- 370 • The results provided by both methods, Staircase and Locati, are comparable, and the Locati  
371 method is more conservative;
- 372 • Applying  $2 \times 10^5$  or  $5 \times 10^5$  cycles per step does not significantly change the fatigue limit  
373 provided by the Locati method. For  $2 \times 10^5$  cycles per step, the results are closer to those  
374 provided by the Staircase method, while being more conservative;
- 375 • The analysis of the Locati tests by method-1 (80% of the stress range in the breaking step) or  
376 method-2 (stress range in the previous step of a resonance frequency drop) provides similar  
377 results. In all cases results closer to those provided by the Staircase method were obtained  
378 using method-2. However, all cases were conservative;
- 379 • The Locati Method is particularly suitable for those cases in which concrete samples are taken  
380 from an existing structure, since it requires extracting less samples;
- 381 • It is concluded that the Locati method is capable of determining the fatigue limit of concrete  
382 similarly to the Staircase method, with the great advantage of significantly reducing the  
383 number of specimens needed. For this reason, it is concluded that the optimum method to  
384 determine the fatigue limit is the Locati Method with  $2 \times 10^5$  cycles per step, since it provides  
385 similar results to the others with a lower number of tests, lower test duration and,  
386 consequently, cheaper procedures.

387 For the valorisation of construction and demolition waste as recycled aggregates in the  
388 manufacture of recycled aggregate concrete, it is necessary to have a wide knowledge about RC  
389 behaviour. In this paper a step has been taken in that direction, optimizing the procedure to  
390 determine the fatigue limit of these concrete mixes.

### 391 Acknowledgments

392 The authors would like to thank the Spanish Ministry of Economy and Competitiveness of Spain for  
393 financing the project MAT2014-57544-R. Also, authors would like to thank to the LADICIM,  
394 Laboratory of Materials Science and Engineering of the University of Cantabria for making available  
395 to the authors the facilities used in this research.

### 396 References

- 397 Alliche, A., 2004. Damage model for fatigue loading of concrete. *Int. J. Fatigue* 26, 915–921.  
398 <https://doi.org/10.1016/J.IJFATIGUE.2004.02.006>
- 399 Bellido de Luna, J., 1989. El cálculo por resistencia a la fatiga en secciones de hormigón armado y  
400 pretensado. *Hormigón y Acero* 40, 77–82.
- 401 British Standards Institution, 2015. Eurocode 2 — Design of concrete structures. Part 1-1 Gen. rules  
402 rules Build. <https://doi.org/10.7773/cm.v27i4.501>
- 403 Carloni, C., Subramaniam, K. V., 2013. Investigation of sub-critical fatigue crack growth in  
404 FRP/concrete cohesive interface using digital image analysis. *Compos. Part B Eng.* 51, 35–43.  
405 <https://doi.org/10.1016/J.COMPOSITESB.2013.02.015>
- 406 Casado, J.A., Carrascal, I., Polanco, J.A., Gutiérrez-Solana, F., 2006. Fatigue failure of short glass fibre  
407 reinforced PA 6.6 structural pieces for railway track fasteners. *Eng. Fail. Anal.* 13, 182–197.  
408 <https://doi.org/10.1016/j.engfailanal.2005.01.016>
- 409 CEN, 2018. EN 14587-1 railway applications - Infrastructure - Flash butt welding of new rails - Part 1:  
410 R220, R260, R260Mn, R320Cr, R350HT, R350LHT, R370CrHT and R400HT grade rails in a fixed  
411 plant.

- 412 CEN, 2016. EN 13230-2: Railway applications - Track - Concrete sleepers and bearers - Part 2:  
413 Prestressed monoblock sleepers.
- 414 CEN, 2014. EN-12390-13 Testing hardened concrete - Part 13: Determination of secant modulus of  
415 elasticity in compression.
- 416 CEN, 2013. EN 80103:2013 Test methods of cements. Physical analysis. Actual density determination.
- 417 CEN, 2011a. EN 197-1 Cement Part 1: Composition, Specifications and Conformity Criteria for  
418 Common Cements.
- 419 CEN, 2011b. EN-12390-3/AC Testing hardened concrete - Part 3: Compressive strength of test  
420 specimens.
- 421 CEN, 2010. EN 14587-2: Railway applications - Track - Flash butt welding of rails - Part 2: New R220,  
422 R260, R260Mn and R350HT grade rails by mobile welding machines at sites other than a fixed  
423 plant.
- 424 CEN, 12390-3:2009, U.-E., 12390-3, E.N., 2009. Testing hardened concrete - Part 3: Compressive  
425 strength of test specimens.
- 426 CEN, 196-6:2010, E.N., 2010. Methods of testing cement - Part 6: Determination of fineness.
- 427 de Azevedo, A.R.G., Alexandre, J., Marvila, M.T., Xavier, G. de C., Monteiro, S.N., Pedroti, L.G.,  
428 2020. Technological and environmental comparative of the processing of primary sludge waste  
429 from paper industry for mortar. *J. Clean. Prod.* 249, 119336.  
430 <https://doi.org/10.1016/j.jclepro.2019.119336>
- 431 Ferreño, D., Casado, J.A.J.A.J.A., Carrascal, I.A.I.A.I.A.I.A., Diego, S., Ruiz, E., Saiz, M., Sainz-Aja,  
432 J.A.J.A., Cimentada, A.I.A.I.A.I., 2019. Experimental and finite element fatigue assessment of  
433 the spring clip of the SKL-1 railway fastening system. *Eng. Struct.* 188, 553–563.  
434 <https://doi.org/10.1016/j.engstruct.2019.03.053>
- 435 Kong, D.J., Xie, C.Y., 2015. Effect of laser quenching on fatigue properties and fracture morphologies  
436 of boronized layer on Cr12MoV steel. *Int. J. Fatigue* 80, 391–396.  
437 <https://doi.org/10.1016/j.ijfatigue.2015.06.024>
- 438 Li, Q., Huang, B., Xu, S., Zhou, B., Yu, R.C., 2016. Compressive fatigue damage and failure  
439 mechanism of fiber reinforced cementitious material with high ductility. *Cem. Concr. Res.* 90,  
440 174–183. <https://doi.org/10.1016/J.CEMCONRES.2016.09.019>
- 441 Locati, L., 1950. *La fatica dei materiali metallici*. Ulrico Hoepli.
- 442 Luo, X.W., Yao, H.L., 2011. Experimental Research on Influence of Loading Method on Dynamic  
443 Behavior of Recycled Concrete. *Adv. Mater. Res.* 199–200, 1171–1174.  
444 <https://doi.org/10.4028/www.scientific.net/amr.199-200.1171>
- 445 Maroušek, J., Strunecký, · Otakar, Stehel, V., 2019. Biochar farming: defining economically  
446 perspective applications 21, 1389–1395. <https://doi.org/10.1007/s10098-019-01728-7>
- 447 Marvila, M.T., Alexandre, J., de Azevedo, A.R.G., Zanelato, E.B., 2019. Evaluation of the use of  
448 marble waste in hydrated lime cement mortar based. *J. Mater. Cycles Waste Manag.* 21, 1250–  
449 1261. <https://doi.org/10.1007/s10163-019-00878-6>
- 450 Maximov, J.T., Anchev, A.P., Dunchev, V.P., Ganev, N., Duncheva, G. V., Selimov, K.F., 2017. Effect  
451 of slide burnishing basic parameters on fatigue performance of 2024-T3 high-strength  
452 aluminium alloy. *Fatigue Fract. Eng. Mater. Struct.* 40, 1893–1904.  
453 <https://doi.org/10.1111/ffe.12608>
- 454 Naseri, H., Jahanbakhsh, H., Hosseini, P., Moghadas Nejad, F., 2020. Designing sustainable concrete

- 455 mixture by developing a new machine learning technique. *J. Clean. Prod.* 258, 120578.  
456 <https://doi.org/10.1016/j.jclepro.2020.120578>
- 457 Opon, J., Henry, M., 2019. An indicator framework for quantifying the sustainability of concrete  
458 materials from the perspectives of global sustainable development. *J. Clean. Prod.* 218, 718–737.  
459 <https://doi.org/10.1016/j.jclepro.2019.01.220>
- 460 Poon, C.-S., Chan, D., 2007. The use of recycled aggregate in concrete in Hong Kong. *Resour.*  
461 *Conserv. Recycl.* 50, 293–305. <https://doi.org/https://doi.org/10.1016/j.resconrec.2006.06.005>
- 462 Sainz-Aja, J., Carrascal, I., Polanco, J.A., Thomas, C., 2019a. Fatigue failure micromechanisms in ed  
463 aggregate mortar by  $\mu$ CT analysis. *J. Build. Eng.* 101027.  
464 <https://doi.org/10.1016/J.JOBE.2019.101027>
- 465 Sainz-Aja, J., Carrascal, I., Polanco, J.A., Thomas, C., Sosa, I., Casado, J., Diego, S., 2019b.  
466 Self-compacting recycled aggregate concrete using out-of-service railway superstructure  
467 wastes. *J. Clean. Prod.* 230, 945–955. <https://doi.org/10.1016/j.jclepro.2019.04.386>
- 468 Sainz-Aja, J., Pombo, J., Tholken, D., Carrascal, I., Polanco, J., Ferreño, D., Casado, J., Diego, S., Perez,  
469 A., Filho, J.E.A.A., Esen, A., Cebasek, T.M., Laghrouche, O., Woodward, P., 2020. Dynamic  
470 calibration of slab track models for railway applications using full-scale testing. *Comput.*  
471 *Struct.* 228, 106180. <https://doi.org/10.1016/j.compstruc.2019.106180>
- 472 Sainz-Aja, J., Thomas, C., Polanco, J.A., Carrascal, I., 2019c. High-Frequency Fatigue Testing of  
473 Recycled Aggregate Concrete. *Appl. Sci.* 10, 10. <https://doi.org/10.3390/app10010010>
- 474 Sainz-Aja, J.A., 2019. Slab track manufacture using out of service railways wastes. PhD Thesis.  
475 University of Cantabria.
- 476 Sainz-Aja, J.A., Carrascal, I.A., Polanco, J.A., Sosa, I., Thomas, C., Casado, J., Diego, S., 2020.  
477 Determination of the optimum amount of superplasticizer additive for self-compacting  
478 concrete. *Appl. Sci.* 10. <https://doi.org/10.3390/app10093096>
- 479 Skarżyński, Ł., Marzec, I., Tejchman, J., 2019. Fracture evolution in concrete compressive fatigue  
480 experiments based on X-ray micro-CT images. *Int. J. Fatigue* 122, 256–272.  
481 <https://doi.org/10.1016/j.ijfatigue.2019.02.002>
- 482 Thomas, C., de Brito, J., Cimentada, A.I.A.I., Sainz-Aja, J.A.J., 2019. Macro- and micro- properties of  
483 multi-recycled aggregate concrete. *J. Clean. Prod.* In press, 118843.  
484 <https://doi.org/10.1016/j.jclepro.2019.118843>
- 485 Thomas, C., de Brito, J., Gil, V., Sainz-Aja, J.A., Cimentada, A., 2018. Multiple recycled aggregate  
486 properties analysed by X-ray microtomography. *Constr. Build. Mater.* 166, 171–180.  
487 <https://doi.org/10.1016/J.CONBUILDMAT.2018.01.130>
- 488 Thomas, C., Setién, J., Polanco, J.A.A., Lombillo, I., Cimentada, A., 2014. Fatigue limit of recycled  
489 aggregate concrete. *Constr. Build. Mater.* 52, 146–154.  
490 <https://doi.org/10.1016/J.CONBUILDMAT.2013.11.032>
- 491 Thomas, C., Setién, J., Polanco, J.A.A., Alaejos, P., Sánchez De Juan, M., De Juan, M.S., Sánchez De  
492 Juan, M., 2013. Durability of recycled aggregate concrete. *Constr. Build. Mater.* 40, 1054–1065.  
493 <https://doi.org/10.1016/J.CONBUILDMAT.2012.11.106>
- 494 Thomas, Carlos, Sosa, I., Setién, J., Polanco, J.A., Cimentada, A.I., 2014. Evaluation of the fatigue  
495 behavior of recycled aggregate concrete. *J. Clean. Prod.* 65, 397–405.  
496 <https://doi.org/10.1016/J.JCLEPRO.2013.09.036>
- 497 Thomas García, C., 2012. HORMIGÓN RECICLADO DE APLICACIÓN ESTRUCTURAL.

- 498 Vicente, M.A., Mínguez, J., González, D.C., 2019. Computed tomography scanning of the internal  
499 microstructure, crack mechanisms, and structural behavior of fiber-reinforced concrete under  
500 static and cyclic bending tests. *Int. J. Fatigue* 121, 9–19.  
501 <https://doi.org/10.1016/j.ijfatigue.2018.11.023>
- 502 Xiao, J., Li, H., Yang, Z., 2013. Fatigue behavior of recycled aggregate concrete under compression  
503 and bending cyclic loadings. *Constr. Build. Mater.*, 25th Anniversary Session for ACI 228 –  
504 Building on the Past for the Future of NDT of Concrete 38, 681–688.  
505 <https://doi.org/10.1016/j.conbuildmat.2012.09.024>
- 506 Zhao, Y., Yu, M., Xiang, Y., Kong, F., Li, L., 2020. A sustainability comparison between green  
507 concretes and traditional concrete using an emergy ternary diagram. *J. Clean. Prod.* 256,  
508 120421. <https://doi.org/10.1016/j.jclepro.2020.120421>  
509

# Fast fatigue method for self-compacting recycled aggregate concrete characterization

*Jose Sainz-Aja<sup>1</sup>, Carlos Thomas<sup>1\*</sup>, Isidro Carrascal<sup>1</sup>, Juan A. Polanco<sup>1</sup>, Jorge de Brito<sup>2</sup>*

<sup>1</sup>LADICIM (Laboratory of Materials Science and Engineering), Universidad de Cantabria. E.T.S. de Ingenieros de Caminos, Canales y Puertos, Av./Los Castros 44, 39005 Santander, Spain.

<sup>2</sup>CERIS, Instituto Superior Técnico, Universidade de Lisboa, Av. Rovisco Pais, 1049-001 Lisbon, Portugal.

\* Corresponding author: carlos.thomas@unican.es

## **Credit Author roles:**

Conceptualization: Jose Sainz-Aja, Carlos Thomas, Isidro Carrascal, Juan A. Polanco; Data curation: Jose Sainz-Aja, Carlos Thomas, Isidro Carrascal, Juan A. Polanco, Jorge de Brito; Formal analysis: Jose Sainz-Aja, Carlos Thomas, Isidro Carrascal, Juan A. Polanco, Jorge de Brito; Funding acquisition: Isidro Carrascal, Juan A. Polanco;; Investigation; Methodology; Project administration: Isidro Carrascal; Resources: Isidro Carrascal, Juan A. Polanco; Supervision;: Carlos Thomas, Isidro Carrascal, Juan A. Polanco. Validation: Jose Sainz-Aja, Carlos Thomas; Visualization: Jose Sainz-Aja, Carlos Thomas; Writing - original draft: Jose Sainz-Aja;; Writing - review & editing: Jose Sainz-Aja, Carlos Thomas, Isidro Carrascal, Juan A. Polanco, Jorge de Brito.

**Declaration of interests**

The authors declare that they have no known competing financial interests or personal relationships that could have appeared to influence the work reported in this paper.

The authors declare the following financial interests/personal relationships which may be considered as potential competing interests: